

Double Gamma Decay in ^{40}Ca and ^{90}Zr

J. Schirmer, D. Habs, R. Kroth, N. Kwong, D. Schwalm, and M. Zirnbauer
*Max-Planck-Institut für Kernphysik and Physikalisches Institut der Universität Heidelberg,
 D-6900 Heidelberg, Federal Republic of Germany*

and

C. Broude
Weizmann Institute of Science, 76100 Rehovot, Israel
 (Received 13 August 1984)

The rare double gamma decay of the first excited 0^+ state in ^{40}Ca and ^{90}Zr has been measured with a segmented 4π NaI detector system, which allows suppression of the perturbing background due to positron annihilation in flight. In both cases the directional correlation of the two photons is found to be asymmetric around 90° , which is explained by an interference of $2E1$ and $2M1$ transitions. The deduced $M1$ quenching factors agree with those from (e,e') and (p,p') measurements.

PACS numbers: 23.20.En, 27.40.+z, 27.60.+j

Many attempts have been made¹ to observe the double gamma decay in nuclei such as ^{16}O , ^{40}Ca , and ^{90}Zr : As these nuclei have a ground and first excited state with spin and parity 0^+ , the first excited state can only decay by internal conversion and pair production or by the simultaneous emission of two γ rays, each with a continuous energy spectrum but summing up to the $0_2^+ \rightarrow 0_1^+$ transition energy. As a result of the small 2γ branching ratio ($\approx 10^{-4}$), these early experiments suffered from insufficient statistics and background problems. In this Letter we present the first unambiguous observation and detailed investigation of the 2γ decay mode in nuclei, which was performed by use of the Heidelberg-Darmstadt "crystal ball,"² a 4π γ -ray detector system comprising 162 individual NaI(Tl) modules. The surprising result of our measurements on ^{40}Ca and ^{90}Zr is that the nuclear 2γ decay proceeds not only via $2E1$ but also via equally strong $2M1$ transitions. The resultant $2M1$ strengths supply an independent measurement of the $M1$ quenching factors deduced from recent (e,e') and (p,p') experiments.³

The 0^+ first excited states⁴ of ^{40}Ca ($E_0=3.35$ MeV, $T_{1/2}=2.1$ ns) and ^{90}Zr ($E_0=1.76$ MeV, $T_{1/2}=62$ ns) were populated via known (p,p') resonances at $E_p=5.08$ MeV and $E_p=7.08$ MeV, respectively, with use of a pulsed beam (0.5 ns width) supplied by the Emperor accelerator of the Max-Planck-Institut. Inelastic protons were detected at backward angles in four surface-barrier detectors, each subtending a solid angle of 0.17 sr; they were mounted together with the metallic targets (^{40}Ca : 0.3 mg/cm², 99.97%; ^{90}Zr : 0.7 mg/cm², 97%) in the center of the "crystal ball" (CB) detector. Special care has been taken to suppress the

perturbing γ background stemming from the decay of the 0_2^+ state via internal pair conversion and the subsequent positron annihilation in flight (PAF). For these events the γ -ray energies $E_{\gamma_1}, E_{\gamma_2}$ and their relative angle θ_{12} are kinematically related by

$$1/E_{\gamma_1} + 1/E_{\gamma_2} = (1 - \cos\theta_{12})/m_e c^2, \quad (1)$$

whereas for the two-quantum decay all relative angles are allowed. Since the angle resolution of the CB is $\pm 9^\circ$, the disturbing PAF events with $E_{\gamma_1} + E_{\gamma_2} = E_{e^+} + 2m_e c^2 \cong E_0$ can be identified by means of Eq. (1) as long as they occur in the CB center. We therefore surrounded the target and the silicon detectors by a small Lucite box of 5-mm wall thickness to ensure that the positrons were either stopped within 5 cm from the CB center or at least sufficiently degraded in energy. In the data analysis we accepted only γ rays which appeared simultaneously but delayed relative to the beam pulse and the inelastically scattered proton $p'(0_2^+)$, thus using the 0_2^+ half-life to reject any prompt background. Moreover, by requiring that two and only two CB detectors fired, it was ensured that each of the two γ rays deposit their energy in one detector only. For the measurement of the linear γ polarization, on the other hand, the CB was used as an 159-fold Compton polarimeter by requiring that one of the two γ rays fired two neighboring detectors. The polarization sensitivity⁵ $Q_c(E_\gamma)$ was measured to be $Q_c(E_\gamma) = 0.53 Q_c^{\text{opt}}(E_\gamma)$, Q_c^{opt} being the sensitivity of an ideal polarimeter.

Figure 1 shows the correlation between the energy E_{γ_1} of one of the two gamma quanta and their relative angle θ_{12} as measured in the ^{40}Ca experiment for two windows on the sum energy $E_{\gamma_1} + E_{\gamma_2}$. For sum energies just below the $0_2^+ \rightarrow 0_1^+$

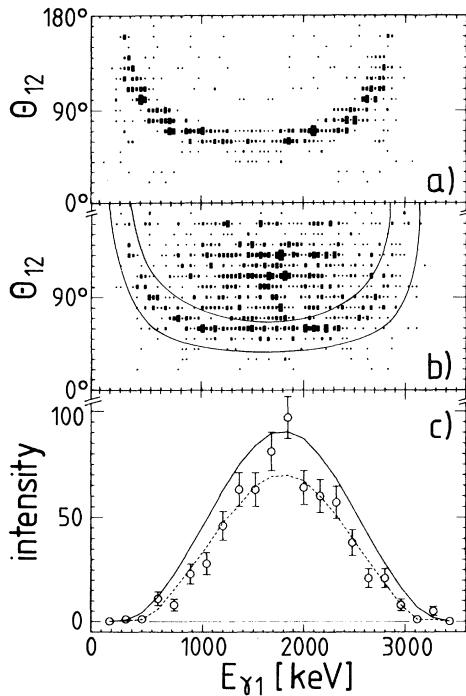


FIG. 1. (a) Correlation between the energy $E_{\gamma 1}$ of one of the two γ rays against their relative angle θ_{12} . The γ rays were measured in delayed coincidence with protons populating the 0_2^+ state in ^{40}Ca (3.35 MeV), requiring $3.05 \text{ MeV} \leq E_{\gamma 1} + E_{\gamma 2} \leq 3.2 \text{ MeV}$. The events are grouped around the kinematical curve expected for positron annihilation in flight (PAF). (b) Same as (a) but for $3.20 \text{ MeV} \leq E_{\gamma 1} + E_{\gamma 2} \leq 3.5 \text{ MeV}$, where the 2γ decay is expected to show up. The region between the two lines is contaminated by PAF. (c) Projection of the matrix (b) on the energy axis excluding the $E_{\gamma 1}$ - θ_{12} region contaminated by PAF. The dashed and solid curves are the expected distributions for double dipole transitions with and without the PAF suppression cut.

transition energy E_0 [Fig. 1(a)] the matrix is dominated by PAF events, whereas for sum energies around $E_0 = 3.35 \text{ MeV}$ [Fig. 1(b)] a strong additional yield appears, which is due to the double gamma decay of the 3.35-MeV state. Figure 1(c) shows the projection of the lower matrix [Fig. 1(b)] on the energy axis $E_{\gamma 1}$, excluding the area between the lines contaminated by PAF. We obtain a continuous distribution peaking at half the $0_2^+ \rightarrow 0_1^+$ transition energy, in agreement with the expected [see Eq. (2) below] energy distribution for double dipole decay. The ^{90}Zr data essentially show the same features.

Figure 2 displays the gamma-ray sum-energy spectra from the 0_2^+ decays in ^{90}Zr and ^{40}Ca . Both spectra are dominated by a strong line at 1022 keV due to positron annihilation at rest, and a continuous PAF background extending up to the 0_2^+ excita-

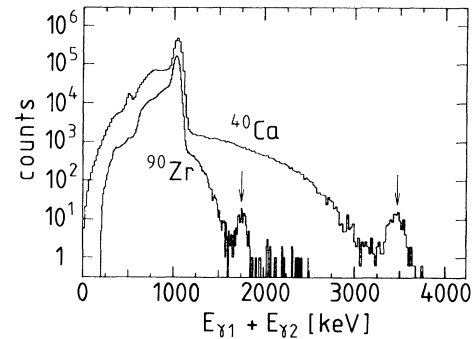


FIG. 2. Sum-energy spectrum measured in delayed coincidence with protons populating the 1.76-MeV 0_2^+ level of ^{90}Zr and the 3.35-MeV 0_2^+ level of ^{40}Ca , respectively, limiting the relative angle θ_{12} and the energy difference between the two γ rays to $120^\circ \leq \theta_{12} \leq 180^\circ$, $|E_{\gamma 1} - E_{\gamma 2}| \leq 0.5 \text{ MeV}$ for ^{90}Zr and $90^\circ \leq \theta_{12} \leq 180^\circ$, $|E_{\gamma 1} - E_{\gamma 2}| \leq 1.8 \text{ MeV}$ for ^{40}Ca . The arrows indicate the expected position of the sum-energy peaks due to the 2γ decay.

tion energy. In both spectra, however, the sum-energy peak due to the double gamma events clearly shows up. In order to obtain such clean spectra the PAF background in the region of the sum-energy peak has been rejected by limiting the relative angle and the energy difference of the two gamma rays as indicated in the figure caption.

Figure 3 shows the directional γ - γ correlation of the double gamma events, suppressing those regions which are deteriorated by PAF. The γ - γ distribution has been corrected for the number of detector combinations contributing to a given θ_{12} , which corresponds to a division by $\sin\theta_{12}$. Traditionally, double gamma decay has been considered

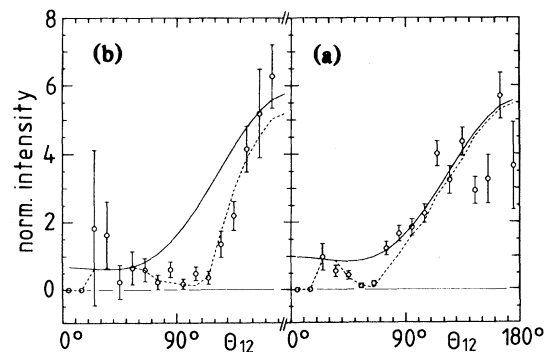


FIG. 3. Directional correlation of the 2γ decay of (a) $^{40}\text{Ca}(0_2^+)$ and (b) $^{90}\text{Zr}(0_2^+)$, excluding the $E_{\gamma 1}$ - θ_{12} region polluted by PAF. The dashed curves correspond to the best fits allowing for $2E1$ and $2M1$ transitions. The solid curves represent the calculated $\gamma\gamma$ correlation if the contaminated area is not excluded.

to be dominated by a $2E1$ process, leading to a γ - γ directional correlation $W(\theta_{12}) \propto (1 + \cos^2\theta_{12})$. The observed correlation, however, is clearly asymmetric around $\theta_{12} = 90^\circ$. This surprising result requires an interference between γ rays of different parities; indeed, it can be explained by a mixture of $2E1$ and $2M1$ transitions, which gives rise to an interference term linear in $\cos\theta_{12}$. As we observe no

indications for contributions from higher multiplicities such as $2E2$ (see below), the spins and parities of the intermediate levels involved in the second-order decay process can be restricted to 1^- and 1^+ . With use of second-order perturbation theory detailed theoretical treatment of the 2γ decay can be found in the literature.^{6,7} Including a linear polarization term, the 2γ correlation function is proportional to

$$W(E_{\gamma 1}, E_{\gamma 2}, \theta_{12}, Q_c) \propto E_{\gamma 1}^3 E_{\gamma 2}^3 \left[\left(1 + \cos^2\theta_{12} - \frac{4\langle 2M1 \rangle \langle 2E1 \rangle}{\langle 2M1 \rangle^2 + \langle 2E1 \rangle^2} \cos\theta_{12} \right) + Q_c(E_{\gamma 2}) \frac{\langle 2E1 \rangle^2 - \langle 2M1 \rangle^2}{\langle 2M1 \rangle^2 + \langle 2E1 \rangle^2} \sin^2\theta_{12} \cos 2\Psi \right]. \quad (2)$$

Here Ψ denotes the angle between the Compton scattering plane and the plane containing the two primary quanta. The reduced matrix elements $\langle 2\sigma 1 \rangle$ are given by

$$\langle 2\sigma 1 \rangle = \langle 0_1^+ || \mathcal{M}(2\sigma 1) || 0_2^+ \rangle = \sum_{\substack{n \\ \nu=1,2}} \frac{\langle 0_1^+ || i^{1-\Lambda(\sigma)} \mathcal{M}(\sigma 1) || n \rangle \langle n || i^{1-\Lambda(\sigma)} \mathcal{M}(\sigma 1) || 0_2^+ \rangle}{E_0 - E_n - E_{\gamma\nu}}, \quad (3)$$

with $\Lambda(E) = 0$ and $\Lambda(M) = 1$, where $\mathcal{M}(\sigma 1)$ are the usual⁵ multipole operators, and E_n denotes the excitation energy of the intermediate state n with spin 1 and parity $(-1)^{1-\Lambda(\sigma)}$. Neither ^{40}Ca nor ^{90}Zr has 1^- or 1^+ levels close to the 0_2^+ state and the double gamma transitions are thus expected to proceed mainly through the corresponding giant resonance states.

To determine the reduced matrix elements the measured γ - γ directional correlation function has been fitted in a first step by use of Eq. (2) with $Q_c = 0$, excluding the region polluted by PAF and taking into account the energy dependence of the NaI peak efficiency as well as the granularity of the CB. The fit results in two equivalent solutions for the ratio $\langle 2E1 \rangle / \langle 2M1 \rangle$, one being the reciprocal of the other. To exclude one of these solutions the linear polarization of one of the two γ rays was measured. By comparing the measured asymmetry ratio

$$R = \frac{W(\Psi = 90^\circ) - W(\Psi = 0^\circ)}{W(\Psi = 90^\circ) + W(\Psi = 0^\circ)}$$

for ^{40}Ca ($R = +0.07 \pm 0.07$) and ^{90}Zr ($R = -0.24 \pm 0.23$) with the expected values of ± 0.04 (^{40}Ca) and ± 0.13 (^{90}Zr), where the $+$ ($-$) sign is for a dominant $\langle 2M1 \rangle$ ($\langle 2E1 \rangle$) matrix element, we conclude that the data for ^{40}Ca and ^{90}Zr are con-

sistent with a dominance of $\langle 2M1 \rangle$ and $\langle 2E1 \rangle$, respectively. Using the observed e^+ rate from the internal pair conversion of the 0_2^+ state to normalize the data, we finally obtain

$$\frac{\Gamma_{\gamma\gamma}}{\Gamma_{\text{tot}}} = (4.5 \pm 1.0) \times 10^{-4}, \quad \frac{\langle 2E1 \rangle}{\langle 2M1 \rangle} = 0.43^{+0.17}_{-0.12}$$

for $^{40}\text{Ca}(0_2^+)$ and

$$\frac{\Gamma_{\gamma\gamma}}{\Gamma_{\text{tot}}} = (1.8 \pm 0.2) \times 10^{-4}, \quad \frac{\langle 2E1 \rangle}{\langle 2M1 \rangle} = 1.9^{+0.7}_{-0.6}$$

for $^{90}\text{Zr}(0_2^+)$. An analysis of the directional correlations including $2E2$ transitions—leading to terms up to $\cos^4\theta_{12}$ —results in an upper limit of $\Gamma_{\gamma\gamma}(2E2)/\Gamma_{\gamma\gamma}(\text{tot}) < 4\%$ for ^{90}Zr and $< 2\%$ for ^{40}Ca . From shell-model estimates an upper limit of $\Gamma_{\gamma\gamma}(2E2)/\Gamma_{\gamma\gamma}(\text{tot}) < 10^{-3}$ is expected.

In the following we first want to show in a qualitative way why in the $0_2^+ \rightarrow 0_1^+$ decay of ^{40}Ca and ^{90}Zr the $2M1$ transitions can successfully compete with the $2E1$ transitions. For ^{40}Ca and ^{90}Zr the first two 0^+ levels can be described to a good approximation⁸ as a complementary mixture of a spherical state $|1\rangle$ and a more complex state $|2\rangle$ involving two or more particle-hole configurations, i.e., $|0_1^+\rangle = \alpha|1\rangle + \beta|2\rangle$ and $|0_2^+\rangle = \beta|1\rangle - \alpha|2\rangle$. The $\langle 2\sigma 1 \rangle$ matrix elements are then given by

$$\langle 2\sigma 1 \rangle = \alpha\beta [\langle 1 || \mathcal{M}(2\sigma 1) || 1 \rangle - \langle 2 || \mathcal{M}(2\sigma 1) || 2 \rangle] + (\alpha^2 - \beta^2) \langle 2 || \mathcal{M}(2\sigma 1) || 1 \rangle.$$

The matrix element multiplied by $(\alpha^2 - \beta^2)$ will be small for both $2E1$ and $2M1$ transitions as the action of

two dipole operators on state $|1\rangle$ generates states which have a very small overlap with state $|2\rangle$. Moreover, the $\langle 1||\mathcal{M}(2E1)||1\rangle$ and $\langle 2||\mathcal{M}(2E1)||2\rangle$ matrix elements will be similar and very nearly cancel each other.⁸ Thus $0_2^+ \rightarrow 0_1^+$ decays via $2E1$ transitions are strongly suppressed in these nuclei. On the other hand, the $2M1$ matrix elements multiplied by $\alpha\beta$ show a quite different behavior: In ^{40}Ca , $\langle 1||\mathcal{M}(2M1)||1\rangle$ is zero as no spin-flip transitions are possible for a spin-saturated configuration, while the corresponding $2M1$ matrix element involving state $|2\rangle$ is of single-particle strength. In ^{90}Zr , where predominantly proton excitations are involved, the same argument applies for the $\langle 1||\mathcal{M}(2M1)||1\rangle$ and $\langle 2||\mathcal{M}(2M1)||2\rangle$ matrix elements in the proton subspace. Thus in both nuclei the $2M1$ transitions are expected to contribute significantly to the $0_2^+ \rightarrow 0_1^+$ 2γ decay.

As a result of the strong cancellation effects a quantitative assessment of the $\langle 2E1\rangle$ matrix element is difficult, quite in contrast to the $2M1$ matrix element. We calculated the detailed structure of the two 0^+ states in ^{40}Ca using an advanced shell-model code⁹ and used published¹⁰ wave functions for ^{90}Zr to determine the theoretical $\langle 2M1\rangle_{\text{th}}$ matrix elements with $M1$ operators for bare nucleons and average experimental³ $M1$ giant resonance energies. Defining a quenching factor γ for the $M1$ strength by $\gamma^2 = \langle 2M1\rangle_{\text{exp}} / \langle 2M1\rangle_{\text{th}}$, we obtain $\gamma = 0.76 \pm 0.05$ for ^{40}Ca and $\gamma = 0.67 \pm 0.09$ for ^{90}Zr , in nice agreement with those values deduced from (e,e') and (p,p') measurements³ [$\gamma_{e,e'}(^{40}\text{Ca}) = 0.87 \pm 0.07$ and $\gamma_{e,e'}(^{90}\text{Zr}) = 0.51 \pm 0.09$ or $\gamma_{p,p'}(^{90}\text{Zr}) = 0.67 \pm 0.09$]. Note, however, that the contributions from the various 1^+ states to the $2M1$ γ decay and inelastic scattering are different. For ^{40}Ca , e.g., mainly one 1^+ level at 10.32 MeV is strongly observed in inelastic scattering; from the known¹¹ branching ratio of this level to

both 0^+ states,

$$\frac{B(M1, 1^+ \rightarrow 0_2^+)}{B(M1, 1^+ \rightarrow 0_1^+)} = 0.43 \pm 0.07,$$

one can calculate that this level only accounts for 15% of the experimentally observed $2M1$ decay. Additional, theoretically expected, 1^+ levels with a weak $M1$ decay to the ground state but a strong $M1$ decay to the first excited 0^+ state contribute to the 2γ decay. Because of the different weightings of the 1^+ states in the inelastic-scattering and, respectively, the 2γ -decay studies—with possible cancellations in the latter—the $2M1$ matrix elements may thus help to differentiate the mechanisms responsible for the $M1$ quenching.

This work was supported in part by the Bundesministerium für Forschung und Technologie.

¹B. A. Watson *et al.*, Phys. Rev. Lett. **35**, 1333 (1975); E. Beardsworth *et al.*, Phys. Rev. **C8**, 216 (1973); Y. Asano and C. S. Wu, Nucl. Phys. **A125**, 557 (1973), and references therein.

²V. Metag *et al.*, Nucl. Phys. **A409**, 331c (1983).

³A. Richter, Phys. Scr. **T5**, 63 (1983).

⁴C. M. Lederer and V. S. Shirley, *Table of Isotopes VII* (Wiley, New York, 1978).

⁵D. Pelte and D. Schwalm, in *Heavy Ion Collisions*, edited by R. Bock (North-Holland, Amsterdam, 1982), Vol. 3, p. 1.

⁶D. P. Grechukhin, Nucl. Phys. **47**, 273 (1963).

⁷J. Eichler, Phys. Rev. A **9**, 1762 (1974).

⁸G. F. Bertsch, Part. Nucl. **4**, 237 (1972).

⁹W. D. M. Rae, Oxford shell-model code, 1982 (unpublished).

¹⁰W. J. Courtney and H. T. Fortune, Phys. Lett. **41B**, 4 (1972).

¹¹K. A. Snover, in *Proceedings of the 1980 Research Center for Nuclear Physics International Symposium on Highly Excited States in Nuclear Reactions* (RCNP, Osaka, 1980).